Front. Environ. Sci. Eng. 2017, 11(2): 2
DOI 10.1007/s11783-017-0907-9

RESEARCH ARTICLE

Effect of electrokinetic property of charged polyether sulfone membrane on bovine serum albumin fouling behavior

Xiaorong Meng[1], Shanshan Huo[1], Lei Wang (✉)[2], Xudong Wang[2], Yongtao Lv[2], Weiting Tang[2], Rui Miao[2], Danxi Huang[2]

1 School of Science, Xi'an University of Architecture and Technology, Xi'an 710055, China
2 School of Environmental & Municipal Engineering, Xi'an University of Architecture and Technology, Xi'an 710055, China

HIGHLIGHTS

- Negatively charged CMPES and positively charged QAPES membranes were fabricated.
- Charge modification reduced the adhesion forces between PES UF membranes and BSA.
- QAPES-BSA *F*/*R* was weaker than that of CMPES-BSA at pH 3 and on the contrary at pH 9.
- Flux decline rate was positively correlated with the adhesion forces of membrane-BSA.
- Variation of adhesion r_0 was consistent with that of ζ potential absolute values.

GRAPHIC ABSTRACT

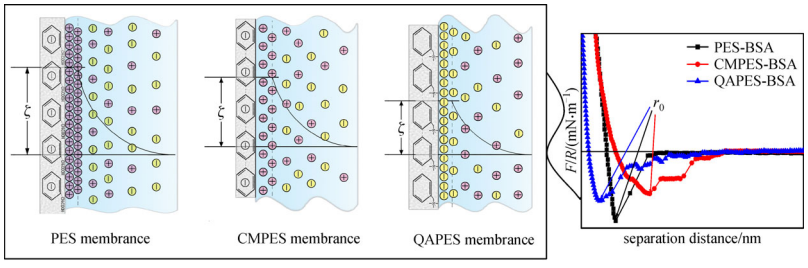

ARTICLE INFO

Article history:
Received 9 October 2016
Received in revised form 31 January 2017
Accepted 6 February 2017

Keywords:
Charged PES UF membrane
BSA
Electrokinetic characterization
Adhesion force
Jump distance

ABSTRACT

Negatively charged carboxymethylated polyethersulfone (CMPES) and positively charged quaternized polyethersulfone (QAPES) ultrafiltration (UF) membranes were prepared by bulk chemical modification and non-solvent induced phase separation method. The effects of PES membrane interfacial electrokinetic property on the bovine serum albumin (BSA) membrane fouling behavior were studied with the aid of the membrane-modified colloidal atomic force microscopy (AFM) probe. Electrokinetic test results indicated that the streaming potential (ΔE) of QAPES membrane was not consistent with its expected *IEC* value, however, within the pH range of 3–10, the ζ potentials of two charged-modified PES membranes were more stable than the unmodified membrane. When pH value was 3, 4.7 or 9, the interaction behavior between charged PES membrane and BSA showed that there was significant linear correlation between the jump distance r_0 of membrane-BSA adhesion force (*F*/*R*) and the ζ potential absolute value. Charged modification significantly reduced the adhesion of PES membrane-BSA, and the adhesion data was good linear correlated with the flux decline rate in BSA filtration process, especially reflected in the CMPES membrane. The above experimental facts proved that the charged membrane interfacial electric double layer structure and its electrokinetic property had strong ties with the protein membrane fouling behavior.

1 Introduction

Charged ultrafiltration (UF) membrane has attracted a wide spread attention in protein separation application area for its excellent sieving property [1]. During the process of separating two proteins, negatively charged organic-inorganic hybrid UF membranes, with controllable electric density and molecular sieving size, possess a better permeability and selectivity compared with unmodified membrane [2–4]. It may be related to some polar functional groups in protein molecular structure such as amino and carboxyl, which are more sensitive to the solution environment, resulting in the fact that their molecular conformation, aggregation size and charge behavior can be easily regulated [5,6].

It has been confirmed that charged membrane has

✉ Corresponding author
E-mail: wl0178@126.com

special separation efficiency for protein. However, membrane fouling remains the main restriction for charged membrane in the application of protein separation technique. Also, there are some contradictory conclusions in associated research. It is considered that the membrane surface charge not only affects the separation performance, but also influences the fouling property. The selectivity and antifouling capacity of the negatively charged blended UF membranes are dramatically enhanced after introducing additive that is high-hydrophilicity and high-charge [3,7]. The polyethylenimine-modified positively charged reverse osmosis (RO) membranes which had been altered the surface charge show the high anti-fouling property to the positively charged foulants [8]. However, different voices did exist, that was the nearly neutrally charged membrane exhibited much better fouling resistance than both the positively and the negatively charged membranes when using bovine serum albumin (BSA), humic acid (HA) and sodium alginate (SA) as the model foulants [9]. Obviously, the main reason for these different research results, on the one hand, because of the simplified design of research work, researchers fail to conduct a more comprehensive or systematic study. On the other hand, the interfacial physicochemical property of amphoteric protein strongly depends on the changing solution environment, the physical and chemical property of membrane interface, especially the electrochemical property of charged membrane, will generate an specific electrokinetic phenomena in different chemical solution environments [10,11], and these changes directly lead to the variability of protein membrane fouling behavior [12].

Researches preliminary obtained the regularity between UF membrane charge behavior and the selective separation by separation data, the macroscopic fouling evaluation means and speculated the interaction between membrane and protein in the specific solution environment through a large number of experimental data. While the charged membrane fouling nature caused by protein is not revealed, for example, the macroscopic membrane fouling phenomena, including flux decay, trans-membrane pressure increase, rejection change and membrane efficiency reduction can't fully reflect the emergence, development and variation of membrane fouling behavior, and the only investigation of these macroscopic phenomena couldn't effectively prevent or mitigate membrane fouling. The study suggests that the instantaneous electrokinetic model can predict the permeate flux and the repulsion of NF membranes is observed with the presence of colloidal particles. The transport of charge particles around the solvent distorts the ionic distribution, resulting in the development of streaming potential and electroosmotic back flow [13]. It seems to lack sufficient research results or techniques to reflect the underlying reasons for membrane-protein interfacial interactions; what's more, little quantitative research has been carried on concerning the charged membrane interfacial behavior and fouling behavior. For example, there is no exploratory conclusion about the contribution among the charge property, charge capacity, including solution condition and other factors on the membrane-protein interaction constitution.

In the last decade, atomic force microscopy (AFM) [14,15] played an important role in the area of revealing the innate character for the formation mechanism of membrane fouling at qualitatively or quantitatively micro-level. AFM technique had been widely recognized in the field of membrane fouling and the technique itself also had been developed meaningfully through this work. While some polymer modification technologies such as blending, copolymerization and grafting was widely employed in modifying charged membrane [2–4,7–9]. These technologies presented new challenges for traditional AFM detection method. Under different pH values, HA, BSA, SA, and their secondary effluent along with its micro forces with polyvinylidene fluoride membrane were effectively determined via membrane or fouling modified AFM colloidal probes. In addition, the determination results verified that pollutants had effect on membrane fouling behavior during the actual filtering process. These results further suggested that the adhesion force of membrane-foulant was the main factor that leads to membrane fouling. Therefore, revealing the relevance between adhesion force and the electrokinetic behavior of charged membrane is important in the further controlling membrane fouling.

Various research means considered that the main factor causing membrane fouling lay in the interfacial interaction of membrane-foulant, as well the charged membrane interfacial electrical double layer (EDL) and its electrokinetic behavior significantly correlated with the solution environment. Obviously, the charged membrane interfacial electrokinetic property inevitably had some impact on protein membrane fouling behavior, while this internal correlation had been little explored in recent research object. Polyether sulfone (PES) UF membranes carrying opposite charges (Negatively charged carboxymethylated polyether sulfone (CMPES) and positively charged quaternized polyether (QAPES)) were synthesized and prepared by bulk chemical modification selecting PES polymer as the membrane matrix in this study. On the basis of the comparative analysis of the correlation between electrokinetic behavior with different electrical charge PES membranes and pH value of solution, setting BSA as the model protein, the relationship between adhesion forces of charged PES membrane-BSA and the interfacial ζ potential was studied by the membrane-modified colloidal AFM probe technique under particular aqueous environments. Meanwhile, this study continues to explore and confirm the membrane fouling behaviors of BSA under different charged form of PES membranes, and hopes to be able to reflect the influence laws of the interfacial electrokinetic behavior of charged membrane on the membrane-protein interaction.

2 Materials and methods

2.1 Preparations of charged PES UF membranes

Polyethersulfone (PES, 105-106, technical grade, BASF chemical company, Germany) was used as membrane material. N-methyl pyrrolidone (NMP, Tianjin Kemel Chemical Reagent Company, China) was employed as the solvent for membrane preparation. Other reagents used in this paper were purchased from Tianjin Fuchen, China, used without further purification.

The carboxymethylated PES was prepared as follows (Eq. (1)), 4 g PES polymer was dissolved in NMP while stirring continuously to obtain a homogeneous solution at room temperature. Then, chloroacetic acid and anhydrous aluminum trichloride were mixed in NMP solution. Next, the mixed solution was obtained for backflow 4 h at 95°C under stirring and nitrogen conditions. After that, the mixture was poured into anhydrous ethanol for precipitation; the product was washed repeatedly by deionized (DI) water. Finally, the carboxymethylated PES was dried for 24 h in the vacuum oven at 60°C before usage.

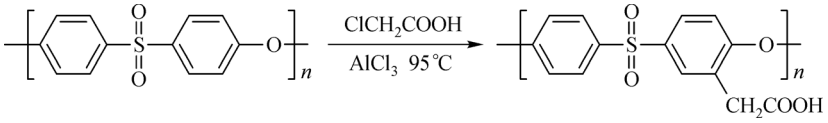

(1)

The preparation of chloromethylated PES was described below (Eq. (2)). First, 20 g PES was dissolved in 1,2-dichloroethane and then the solution was stirred and heated to 60°C. Next, prepare the complex solution by dissolving 1.5 g zinc chloride into 20 g chloromethylether. The total amount of the prepared solution was added into PES solution, and the reaction was carried out at 60°C, taking about 6 h and later cooled to room temperature. Afterwards, the polymer solution was gradually precipitated into hot water under mechanical agitation. Finally, chloromethylated polymer was precipitated from solution, and went through the process of filtering, washing for several times with deionized (DI) water and then dried under vacuum environment at 60°C for 24 h.

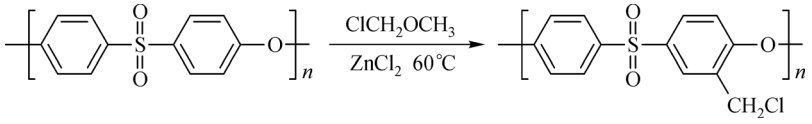

(2)

Flat sheet PES UF membranes were prepared by non-solvent induced phase separation method [16]. The five kinds of PES membrane casting solution were prepared at 60°C in a container, the composition of which were given in Table S1 of the supplementary material. The polymer solution was stirred continuously with a stirrer to discharge air bubbles, and then kept for one day and cast onto a flat glass. After 5 s, the resultant membrane was peeled from the glass in DI water. Therefore, the PES, carboxymethylated PES (CMPES) and chloromethylated PES (CCPES) membranes were acquired. Thereinto, the CCPES membrane was immersed into 30 wt% trimethylamine solution for 48 h to induct quaternary groups into the membrane. The membrane was then put into 1 $mol \cdot L^{-1}$ NaOH solution for 24 h (Eq. (3)). At last, to remove the remaining solvent, the quaternized PES (QAPES) membrane was obtained and washed for several times with DI water, and kept it in DI water before testing.

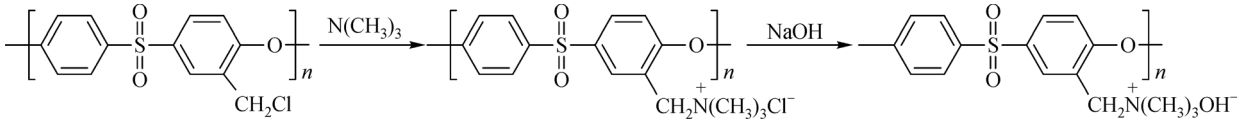

(3)

2.2 Membrane characterizations

The chemical compositions of three representative PES membranes were measured by the fourier transform infrared (FT-IR, IRprestige-21, SHIMADZU, Japan) [17]. Scanning electron microscopy (SEM, JSM5800, JEOL, Japan) was used to observe the surface and cross-section morphology of membrane [18]. At least 5 replicates were carried out for each type of membrane sample.

Pure water flux (25°C, DI water, constant dead-end membrane filtration setup, operating pressure 0.1 MPa) and BSA rejection (pH = 7, feed BSA concentration 1 $g \cdot L^{-1}$, operating pressure 0.1 MPa) were to characterize the membrane permeability [19]. The porosity (ε) and average pore radius (r_m) of membranes were determined by gravimetric method and filtration velocity method based on Guerout-Elford-Ferry equation, respectively [20]. Water contact angle (*WCA*) expressed membrane surface hydrophilic and hydrophobic property (ultrapure water, 25°C) [21]. Six measurements were conducted of membranes and the average values were reported. The ion

exchange capacity (*IEC*) of charged PES membranes was respectively determined quantitatively by back titration method following Ref [22].

2.3 Electrokinetic characterizations

2.3.1 Membrane streaming potential

In the electrolyte solution with different ionic strength, the electric double layer structure and density of charged membrane on both sides were varied accordingly. Under the specific pressure, electric double layer of membrane interface dissociate to form a different streaming potential (ΔE). ΔE of five PES membranes was measured with the homemade ΔE apparatus (Fig. S1 of the supplementary material). Ultrapure water (resistivity was 18.2 MΩ.cm) was used to prepare the electrolyte solution (1–5 mmol·L^{-1} KCl) and maintained at 25°C. ΔE was measured at 5 pressures in the range of 0.01–0.05 MPa. The membranes needed to be rinsed by DI water and be pre-compacted at 0.1 MPa to minimize the deviation caused by swelling before usage.

The process was as follows: KCl was slowly injected into the cavity for removing bubbles before measurements. First, the initial pH of the background electrolyte solution was adjusted to pH 3 by HCl. Then, solution pH value was increased to 10 in small steps by adding KOH by PHS-3C pH meter (Shanghai, China) at 25°C. ΔE at each pH was directly obtained by reading the value that displaced on the voltmeter after stabilization. Pressure was supplied by nitrogen tank and the electrode calibration was taken before each measurement. The potential difference was measured 10 times and a mean value was calculated.

2.3.2 ζ potential

ζ potential of charged PES membranes was determined from electrophoretic mobility measurements with the ΔE slope versus pressure plots based on the well-known Helmholtz-Smoluchowski Eq. (4) [23]:

$$\zeta = \frac{\Delta E \mu \eta}{\Delta P \varepsilon}, \tag{4}$$

here, ζ is zeta potential, ΔE is streaming potential, ΔP is the applied pressure, ε is the dielectric constant, μ and η are the conductivity and viscosity of the solution, respectively.

2.4 Preparation of BSA solution

The organic foulant chosen to represent protein was BSA (Mw = 67 kDa, Sigma Chemical Co., USA). BSA had an IEP around pH 4.7 [24] and the stock solution was 1 g·L^{-1}. Then BSA solution was performed for 24 h to ensure the complete dissolution and stored in sterilized glass bottle at 4°C. Before carrying out ultrafiltration experiments, the pH value of BSA solution was adjusted to 3, 4.7, 9 with addition of 0.1 mol·L^{-1} NaOH or HCl solution.

2.5 Ultrafiltration experiments

All the ultrafiltration experiments were performed using charged PES membrane with an effective membrane area of 28 cm^2, and a laboratory-scale dead-end membrane filtration setup was employed for the experiments [14]. Each fouling filtration process needs a clean membrane, and the BSA concentration was 20 mg·L^{-1}. The normalized flux (J/J_0) was used to analyze the BSA fouling behavior under the influence of different solution pH values.

2.6 Adhesion force measurements of BSA-charged membranes

The preparation of AFM colloidal probe and the adhesion force measurements were carried out based on previous study [15]. AFM adhesion force measurements were performed under contact mode, by injecting the BSA solution (pH = 3, 4.7, 9) in a fluid cell. The prepared colloidal probes were used as PES, CMPES or QAPES membranes to measure the adhesion forces between the membrane itself and BSA-fouled membranes, respectively. The force measurements were obtained at 6 different locations, and 10 force measurements were taken at each location.

3 Results and discussion

3.1 Membrane composition and morphology

FT-IR spectra of three representative PES membranes were presented in Fig. 1. The peak at 3066 cm^{-1} is associated with the C-H stretching vibration absorption of aromatic hydrocarbon, the sharp peak at 1589 cm^{-1} is the skeletal vibration absorption of aromatic hydrocarbon. The peak at 1360 cm^{-1} is ascribed to the asymmetric stretching vibration absorption of S = O bond, the peak at 1668 cm^{-1} is identified to the asymmetric stretching vibration absorption of C = O bond. The spectrum of modified PES membrane shows a wide band (at 3447 cm^{-1} in Fig. 1(b)) which is attributed to the stretching vibration of O-H or N-H bond. The peaks within ranges of 2880 to 2995 cm^{-1} are respectively attributed to the bending vibration of-CH_2 groups. The characteristic peak appearing at 2364 cm^{-1} in the spectrum of QAPES-2 is ascribed to the bands of the quaternary ammonium group. In the FT-IR spectra of CMPES-2 membrane, the associative absorbing peaks at 1500–1700 cm^{-1} of carboxyl functional groups are obvious. The associative absorbing peaks near 3400 cm^{-1} belongs to the stretching vibration of O-H groups of CMPES-2 and QAPES-2 membranes. These characteristic absorptions suggest that the charge function groups have

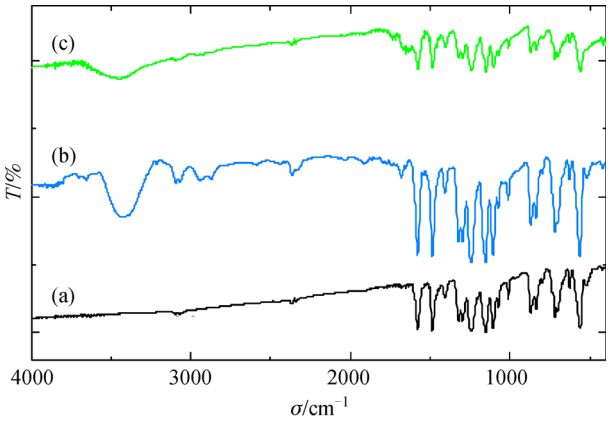

Fig. 1 FT-IR spectra of three representative PES UF membranes: (a) PES, (b) QAPES-2, (c) CMPES-2

been successfully introduced into the PES.

Surface and cross-section electron microscopy images of five membranes are shown in Fig. 2. All the cross-sectional morphologies demonstrate the unique asymmetric structure of non-solvent induced phase separation method, including dense or porous cortex and well-developed cross-section finger-like pores. Among them, the surface of PES membrane is porous, cross-section finger-like pores are clear, and the supporting layer is dense. However, the surfaces of CMPES membrane and QAPES membrane are relatively dense, the cross-section finger-like pores are densely distributed, and the supporting layer is relatively loose. This can be related to the different exchange rates of solvent (NMP) with non-solvent (DI water) for the unequal polar casting solution in the phase separation process. The rapid solidification of PES membrane skin layer prevents

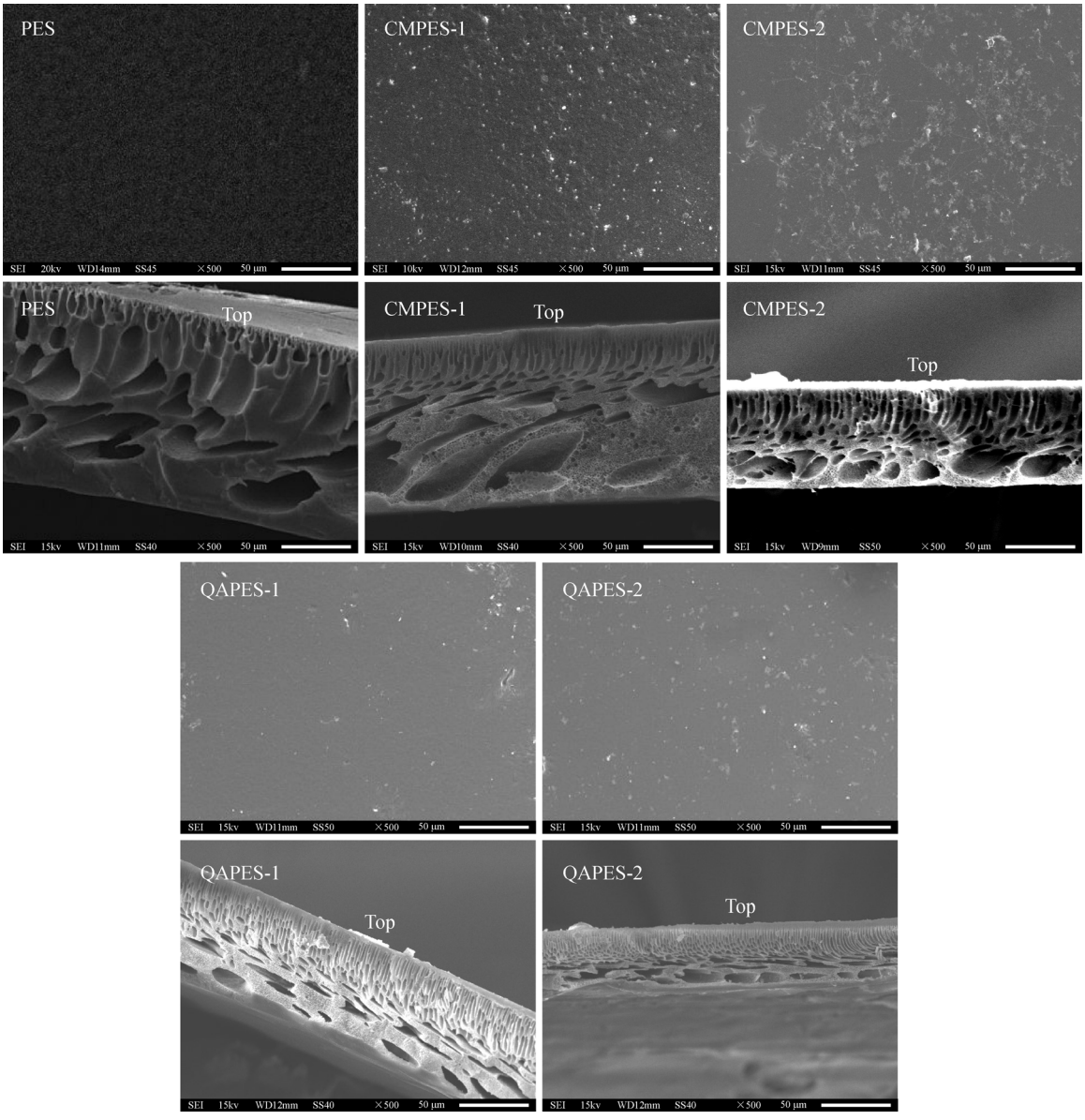

Fig. 2 Surface and cross-section SEM images of five PES UF membranes

coagulation bath (DI water) entering into the membrane matrix, thus retards the solvent-non-solvent exchange rate and eventually causes the growth of polymer-rich phase behavior inside membrane and the instantaneous phase separation obviously, which forms finger-like pores. The charge-modified membrane contains polar functional group, which has good compatibility with coagulation bath. Thus, during the phase inversion process, the non-solvent can quickly enter into membrane interior through the skin layer and form a coexisting phase inversion process together with instantaneous and delayed phase separation, so the finger-like pores become smaller and possess the characteristic of relatively porous cross-section and loose supporting layer [25]. As shown in Fig. 2, the finger-like pores of the CMPES-2 membrane are denser than those of the CMPES-1 membrane, but due to the low degree of chloride methylation, and the quaternary ammonium reaction occurred on the surface of the membrane, the SEM morphology difference of the two QAPES membrane are smaller. Figure 2 shows that the mechanism of charge modified PES is different, there are some differences in the membrane surface and the internal structure. Although some literatures found that the dense structure formed on the UF membrane surface would help to prevent foulants depositing on the membrane surface or blocking membrane pores, while the relevant expression about the UF membrane surface roughness in terms of the antifouling was not consistent [26,27].

For the basic property parameters of five membranes, see Table 1.

Table 1 data shows that influence of the chemical composition and structure of the membrane material, the permeability performance, structural parameters, *WCA* and *IEC* values of the five kinds of PES membrane present great differences. The *WCA* value of charge-modified CMPES membrane and charge-modified QAPES membrane decrease dramatically compared with that of PES membrane. It turns out that the polarity of PES is enhanced after charge-modified process, the order of *IEC* value is CMPES>QAPES>PES. Preliminary shows the difference of the number of free flowing charge in various PES membranes.

3.2 Electrokinetic characterization

The membrane-liquid interface will form a special electrokinetic phenomenon when the electrolyte solution flows through the charged membrane surface. Wherein ΔE is the potential difference across membrane surface where there zero net charge flows through membrane and the ΔE can be integrated to reflect the charge information of membrane skin, transition and support layers. Determination of ΔE can reflect the interfacial electrokinetic parameters such as ζ potential and charge density. Figure 3(a) shows ΔE of five charged PES membranes measured in 3 mmol·L^{-1} KCl solution and 0.01–0.05 MPa (the three series of charged PES membrane, the relationship between ΔE and the change of pressure in 1–5 mmol·L^{-1} KCl solution are shown in Fig. S2 of the supplementary material). Absolute values of ΔE of five PES membranes increase as the operating pressure increase. This is because that the increase in trans-membrane pressure may lead more charge particles to be dissociated from the EDL of the membrane. The absolute values of ΔE of five membranes increase in the following order: QAPES-2 < QAPES-1 < PES < CMPES-1 < CMPES-2. The ΔE of CMPES membrane is negatively charged because of introducing carboxyl functional group, it's also easy to find the validity of negatively charged modification according to its relatively high *IEC* value. While ΔE of the unmodified PES membrane is negative and is relatively higher than the value of QAPES, which may be related to the fact that there are many electron-rich aromatic rings within PES membrane. As aromatic rings possess better supplied character, it could make the positive ions of electrolyte solution as counter ions to form an adsorbed layer in membrane interface, as well as the negative ions as common ions to the diffuse layer. The counter ions and common ions together constitute the EDL structure of PES membrane and result in its ΔE significantly negative. Similarly, QAPES membrane's absolute value of ΔE reaches its minimum, which indicates that its net charge density in structure of electrical double layer reaches its lowest. QAPES membrane which has been positively charge-modified offsets PES intrinsic electronegativity and still shows the positive ΔE value over the entire studied pH ranges. It also explains why the absolute value of ΔE QAPES is low but the *IEC* value is relatively high (Table 1). And the ΔE of the two QAPES membrane is close, not only because of the low degree of chloride, but also related to the quaternary ammonium reaction occurring only on the membrane interface. The following picture shows the structure of electrical double layer of three representative PES membranes.

Table 1 Interfacial and structural parameters of charged PES UF membranes

types	J /(L·m^{-2}·h^{-1})	R_{BSA} /%	ε /%	r_m /nm	*WCA* /(°)	*IEC* /(mmol·g^{-1})
PES	76.24	87.82	70.71	43.67	85.71	0.11
CMPES-1	175.72	89.27	72.40	46.12	69.40	2.81
CMPES-2	333.87	90.16	80.24	48.21	44.30	4.13
QAPES-1	176.11	95.02	65.01	59.20	79.50	1.08
QAPES-2	243.03	95.12	81.43	51.10	70.86	1.43

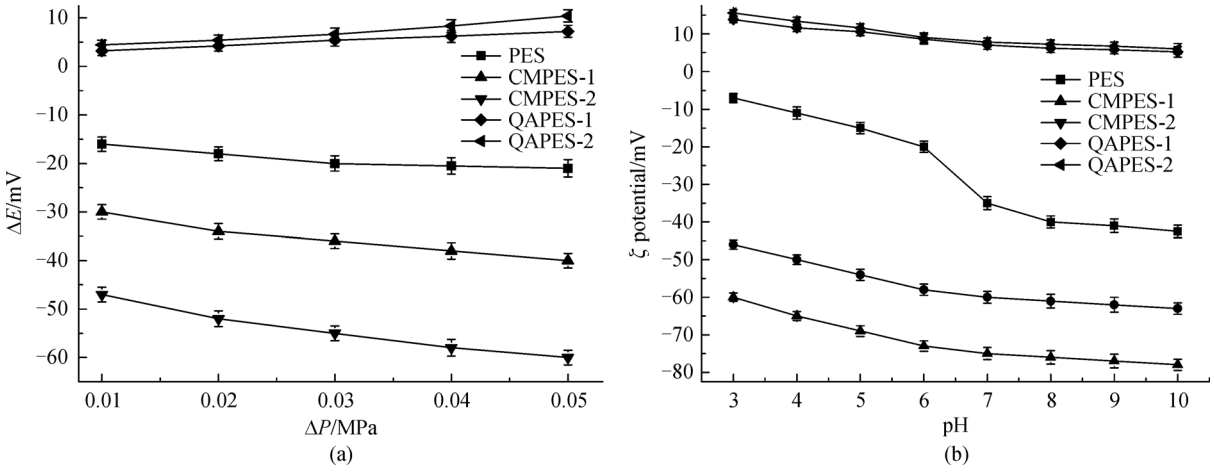

Fig. 3 Electrokinetic characterization of five PES membranes: (a) streaming potential as a function of pressure and (b) ζ potential as a function of pH (KCl concentration: 3 mmol·L^{-1}, $T = 25$°C, pH = 3; $\Delta P = 0.03$ MPa)

According to ΔE under different pH conditions, ζ potential of five membranes are shown in Fig. 3(b). Based on EDL theory, ζ potential of membrane interface expresses the electric potential difference between the "slipping plane" where the aqueous solution relatively move from the membrane surface by a distance and the interior of the liquid [28]. ζ potential value and the response to solution environment can reflect the charge property and stability of EDL on the membrane surface [29]. Figure 3(b) shows that ζ potentials of PES and CMPES membranes are both negative at the solution's pH value from 3 to 10, while the ζ potential of QAPES membrane is positive throughout the entire studied pH ranges.

ζ potential of PES membrane is intensively changing with solution's pH value since the low free-flowing charge number formed on PES membrane surface. QAPES and CMPES membranes perform smooth responses to the changes of solution pH, it illustrates that membrane surface after charge-modified process forms a more stable EDL structure which can withstand the impact of the charge particles in external solution environment on the membrane charge behavior. The positively charged QAPES membrane is significantly response to alkaline environment, while the negatively charged CMPES membrane has an outstanding responsiveness to acidic environment. This phenomenon can be explained by that large numbers of hydrogen ions in acidic environment or hydroxide ions in alkaline environment result in the selective effects for counter ions in charged membrane interfacial EDL. The different charged membranes in terms of the significant differences in electrokinetic characterization have different response characteristics to the ambient condition; this change will affect the interactions between membrane interface and the protein particles, and eventually lead to different fouling behaviors of amphoteric protein during filtration process at different solution environments.

Figure 4 expresses the schematic structure of three PES membranes interfacial electric double layers according to the *IEC*, ΔE and ζ potential values. CMPES membrane interface has the higher *IEC* value, and the larger ΔE and ζ potential absolute values, it illustrates that CMPES membrane possesses a more denser and stable electric double layer structure and organization. Even if QAPES

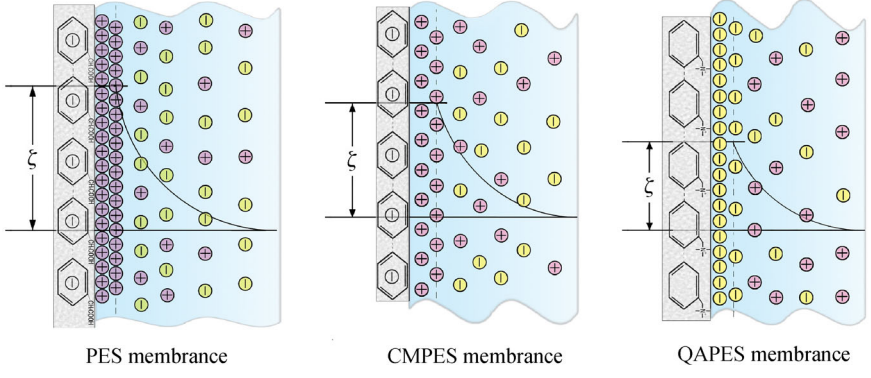

Fig. 4 Electrical double layer structure and electrokinetic property of three membranes

membrane has relatively high *IEC* value after positively charged-modified process, while due to the fact that QAPES membrane should offset the electronegativity on aromatic rings of PES backbone, its net value of positive charge decreases and double electric layer structure attenuates, ΔE and ζ potential absolute values are relatively small. However, compared with the relatively loose double electric layer structure of PES membrane, the ionic layer of QAPES membrane is denser and makes great contribution to EDL's stability.

3.3 UF membrane flux decay

Figure 5 shows the normalized flux decline curves of three PES UF membranes at different solution pH environments during BSA operation. (Since the two CMPES and two QAPES flux decay trend are similar, the figure shows only the data of CMPES-2 and QAPES-2 as the representative) The changes of normalized flux decline rates (J/J_0) in BSA filtration process are very similar under different pH values. All of the decay curves show a sharp flux decline in the initial 30 min and a gentle decay 30–60 min. This phenomenon is in agreement with the result in our previous study that the membrane fouling behavior mainly occurs in the early filtration stage caused by the strong adsorption effect between BSA and membrane surface [14]. It indicates that the first problem for controlling the BSA membrane fouling is to eliminate the adsorption between membrane and BSA.

Figure 5 also shows that the J/J_0 of three membranes reaches its strongest at pH 4.7 (the IEP of BSA). This observation is consistent with the findings of Palecek's group [30], who used PES microfiltration membrane to respectively filtrate five kinds of proteins and found that the more of pH deviating from IEP, the greater of protein membrane filtration flux. At the same time, there are some noteworthy phenomena: the largest flux decay of BSA occurred on the uncharged modified PES membranes at each pH value. The flux decay rate of QAPES and CMPES membranes appear cross before and after the IEP of BSA, J/J_0 of CMPES is much higher than that of QAPES at pH 3 and on the contrary at pH 9. This is because the charging behaviors of BSA below and above the isoelectric point are different, thus the reactions between BSA and interface of charged membrane with different electric double layer structure are different in the corresponding pH environment. For example, BSA is positively charged in pH 3, so it is mutually exclusive with the same electropositive QAPES, and the result is that the adsorption quantity of BSA on the membrane surface is small, which in turn leads to low degree of membrane fouling and slight trend of flux decay. However, the positively charged BSA attracts with the opposite charged CMPES, which causes the adsorption capacities to strengthen and the membrane fouling behavior to accelerate. Similar phenomena did exist in the early literature, but most of the literature only explain this phenomena through the change of BSA interfacial charge under different water environment [31,32].

3.4 Microscopic forces

The microscopic interfacial forces generally is a comprehensive combination of electrostatic interactions, hydrogen bonding, van der Waals interactions, EDL interactions and other forces caused by chemical bonds or acid-base interactions; in addition, hydrophobic and steric interactions may be important [33]. In this study, three kinds of membranes were modified by AFM colloid probe to reflect the micro force between the interface of PES and the BSA. Figure 6 shows the adhesion forces between three membranes and BSA and the corresponding frequency distributions of F/R at different pH values. A force-distance curve is divided in two parts, the approach and the withdrawal curve. Both parts can be further divided into discrete zero lines and contact lines, which are respectively named as jump-to-contact in the approach curve and

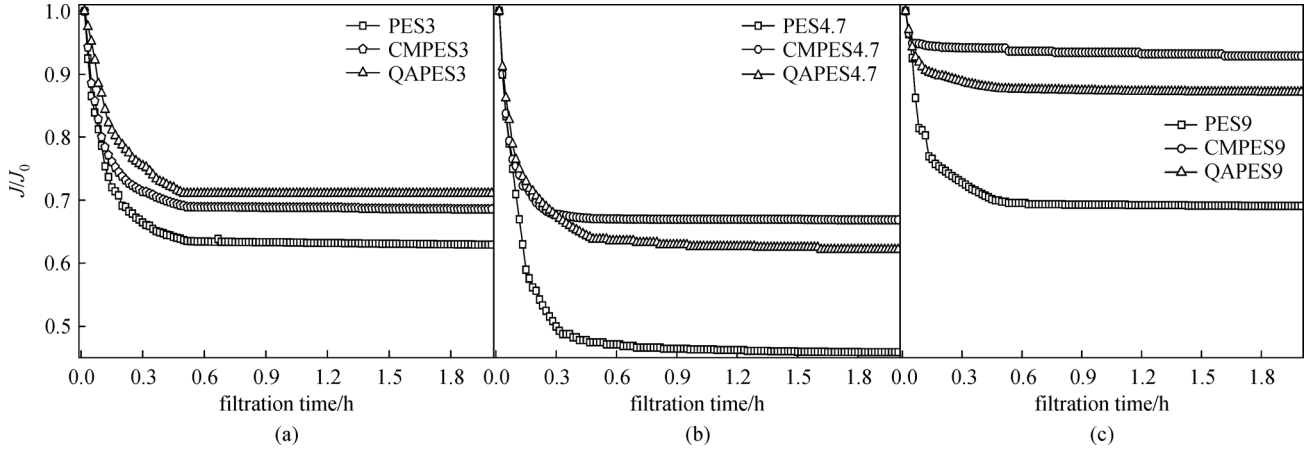

Fig. 5 Normalized flux decline curves for BSA solution as a function of time at different pH values (Experimental conditions: applied pressure, 0.1 MPa; test temperature, 25°C) (a) pH = 3, (b) pH = 4.7, and (c) pH = 9

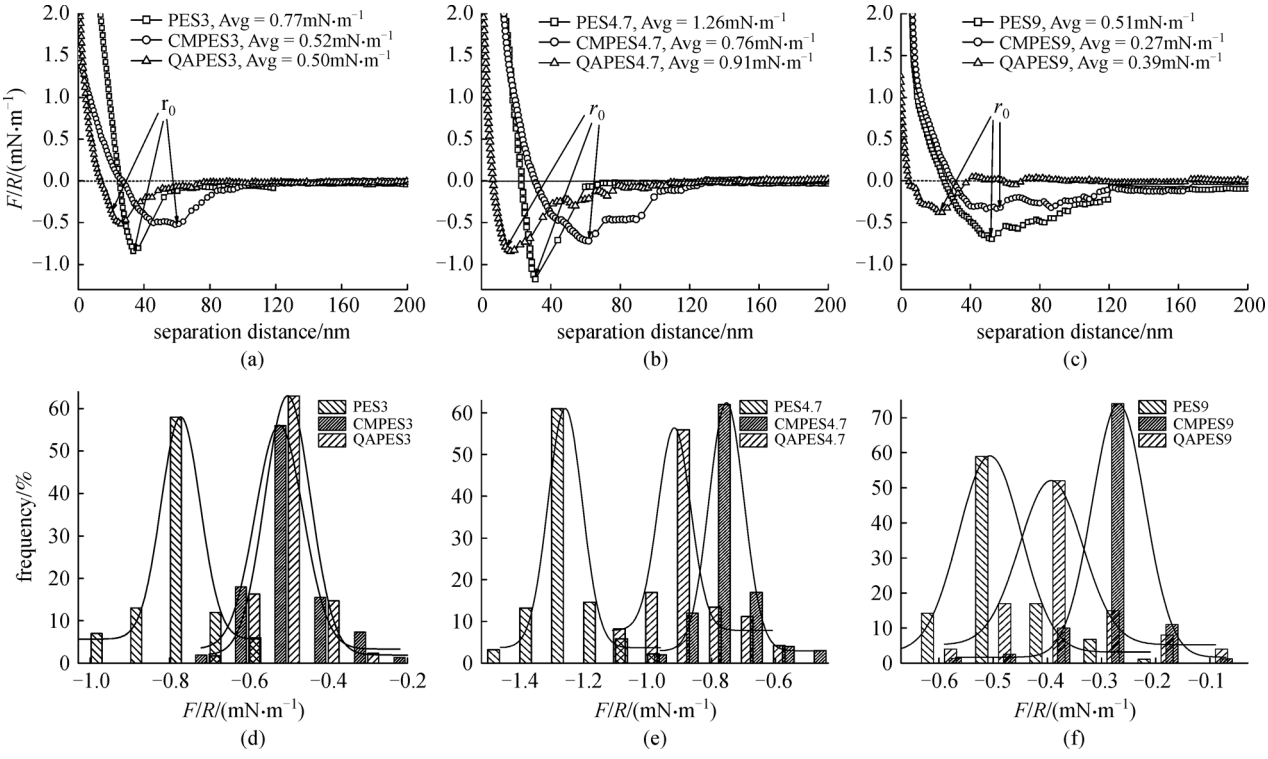

Fig. 6 Adhesion forces of BSA on PES, CMPES, QAPES UF membranes ((a) pH = 3, (b) pH = 4.7, and (c) pH = 9) and the corresponding frequency distributions of F/R ((d) pH = 3, (e) pH = 4.7, and (f) pH = 9) at different pH values

jump-off-contact in the withdrawal curve. r_0 expresses the jump distance that the jump-to-contact occurs at the distance, where the gradient of the attractive force exceeds the elastic constant of the cantilever, so that the tip snaps onto the sample surface [34]. So r_0 should be related to the charged membrane EDL structure and charge density.

It can be seen from Fig. 6 that the r_0 of membrane-BSA adhesion force increases in following order: QAPES < PES < CMPES. When both the EDL thickness and charge density increase, that is, the membrane interfacial electrokinetic parameters ζ and ΔE absolute values get larger, r_0 will correspondingly increase for the shielding effect of the EDL. Comparing with Figs. 3 and 6, the variation of r_0 is basically consistent with that of the electrokinetic property parameters of ζ potential and ΔE absolute values (Electrokinetic Characterization Section) of three membranes, which basically illustrates the membrane interfacial EDL structure will directly influence the jump distance of the interfacial membrane-foulant interactions.

The adhesion forces are the main factors causing membrane fouling behavior [14]. When at pH 4.7, carrying net charges and electrostatic interaction force of BSA approach to zero, thus, the adhesion force at pH 4.7 is the strongest. Also the adhesion force of PES-BSA is the strongest which may be mainly attributed to nonspecific protein adsorption and deposition on the surface or in the pores of the membrane by hydrophobic interaction between the highly hydrophobic PES and the hydrophobic parts of BSA [35]. On the contrary, the lower adhesion forces between CMPES, QAPES membranes and BSA can be explained by the strong electrostatic repulsion [7].

Meanwhile, the adhesive power's rule is different from CMPES and QAPES membrane with BSA which modified by charge in the solution environment which has diverged from isoelectric point, among them, the adhesion force of QAPES-BSA is weaker than that of CMPES membrane-BSA at pH 3 and on the contrary at pH 9. This measured data is consistent with the BSA flux decline trend at both membranes. A similar observation has been reported in Miyama's studies, it is expected that mutual electrostatic interactions between membrane and BSA will be repulsive above the IEP, ignorable at the IEP, and the stronger electrostatic attractions at pH below the IEP [32]. The repulsion electrostatic interactions could be formed between the positively charged BSA and the positively charged QAPES membrane at pH 3. At pH 9, (i.e. above the IEP of BSA) there is an electrostatic attraction resulting in an overall attraction between the two surfaces. This change behavior seems not to only be explained by electrostatic and hydrophobic interaction; alternatively, the electrokinetic phenomena such as charged membrane interfacial ζ potential, ΔE and the certain existing correlation between EDL structure and the membrane-foulant interaction behavior should be forced.

In Section 3.2, the EDL structure of 3 types of PES membrane interface and the solution was studied and

explained. It can be found that the EDL stability of PES membrane interfaces are different and electrostatic interactions between the given BSA charges and membranes are not the same due to the EDL structure differences on PES membrane surface in different aqueous environments according to Figs. 3(b) and 4. A denser double electrode layer charge barrier is formed for CMPES and QAPES. It's not only has high stability in chemical environment (pH there) of solution (expressed as in Fig. 3 as shown ζ potential relatively stable change process with pH), but also has effect on weakening interaction force of membrane-BSA. This can be verified by r_0 variation in Fig. 5, also be reflected by adhesion data in Fig. 6. The physicochemical properties of BSA have more sensitive response to solution environments. Since the physicochemical property of protein, it's more sensitive to the solution environment. Charged membrane and physicochemical property of protein can have effect on microscopic interfacial behavior directly, and then, it can affect selective permeation and membrane fouling of protein on charged ultra-filtration membrane. Therefore, it's possible to achieve the aims that adjust and optimize the ultrafiltration process of protein by setting particular solution chemical environment to change microscopic interaction force between charged membrane and pollutant.

3.5 Linear correlations analysis

Compared with the microscopic forces studying data, it can be easily found that J/J_0 is highly consist with AFM adhesion force data, even the adhesion force is closely related to the charged PES membrane interfacial electro kinetic property. Flux decline for all BSA-fouled membranes mainly occurred during the filtration period of 0–1 h, which may be caused by the rapid adhesion force of fouling and the membranes. To analyze the formation of membrane fouling and confirm the relationship between the BSA membranes fouling behavior and the solution chemical property and the charged membrane interfacial electro kinetic property, the linear fitness between adhesion force (F/R) and membrane initial flux decline rate ($\Delta(J/J_0)/t$), the jump distance r_0 of membrane-BSA adhesion forces and the ζ potential at pH 3, 4.7, 9 have been carried out. The correlation coefficients are respectively 0.8914 and 0.8462 in Fig. 7. The high correlation coefficients once again confirmed that the charged membrane-modified AFM probes which truly reflected the interfacial electrochemical property of membrane could accurately analyze membrane fouling behavior. A good linear relationship between r_0 and ζ potential in Fig. 7 further indicated that the electro kinetic property parameters such as charged membrane EDL constitution and structure under certain environments had the necessary connection with membrane fouling behavior, as well as the significant impact on the formation of membrane fouling.

4 Conclusions

The preparation of positively and negatively charged PES UF membranes are applied to studying the relationship between membrane fouling and interfacial charged behavior in the process of protein separation. ΔE and ζ potential of CMPES and QAPES membranes were obtained by transmissible membrane potential testing technology. According to the further research, the ΔE and the ζ potential absolute values of three charged PES membranes rises along with the increasing of pH when pH of solution changed from 3 to 10. At the same time, the variation tendency and range are closely related to the charged membrane interfacial EDL structure and the charged density. The adhesion force of membrane-BSA molecule at pH 4.7 is the strongest for net charges and the zero electrostatic interaction force. In addition, the adhesion forces between CMPES and QAPES membrane and BSA

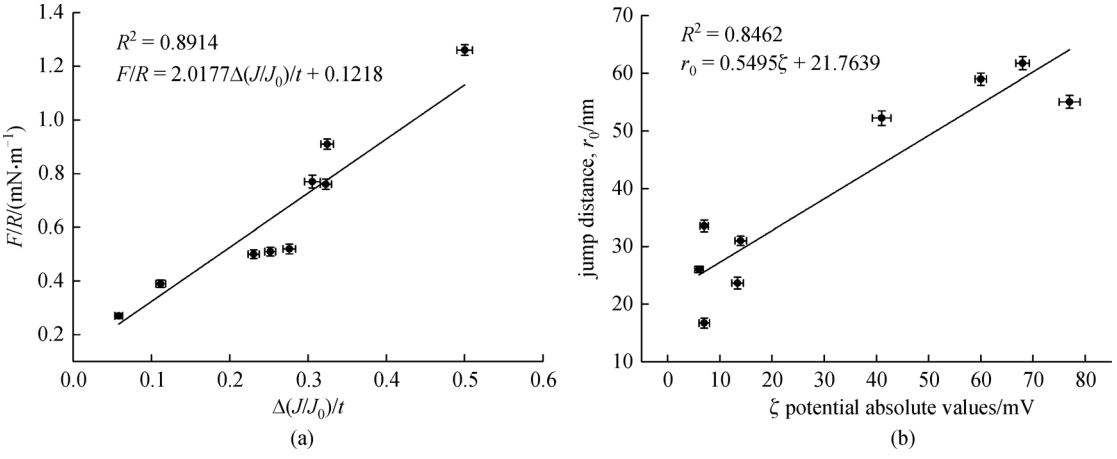

Fig. 7 Linear correlations analyses: (a) adhesion force (F/R) of membrane-BSA and normalized flux decline rate ($\Delta(J/J_0)/t$) during the initial 1 h filtration and (b) the jump distance r_0 of F/R and ζ potential at pH 3, 4.7, 9

are weaker than that of PES in each single pH value because of declining interfacial hydrophobicity, higher ion exchange capacity, and more stable structure of double electrode layer. The adhesion forces between membrane and BSA (F/R) and the flux decay rate ($\Delta(J/J_0)$), jump distance (r_0) of F/R the interfacial ζ potential has related coefficient (0.8772 and 0.8318). It can be proved that the relevance among charged membrane interfacial electro kinetic property, microscopic adhesion forces of membrane-BSA and membrane fouling behavior, which proved that the charge density, EDL structure and stability of charged membrane interface had an improvement for protein membrane fouling behavior to a certain extent in a suitable solution environment.

Acknowledgements This research was supported by Innovative Research Team of Xi'an University of Architecture and Technology; the National Natural Science Foundation of China (Grant Nos. 51178378 and 51278408) and the Youth Science Foundation Project (No. 21607118).

Supplementary material is available in the online version of this article at http://dx.doi.org/10.1007/s11783-017-0907-9 and is accessible for authorized users.

References

1. Li Q, Bi Q Y, Lin H H, Bian L X, Wang X L. A novel ultrafiltration (UF) membrane with controllable selectivity for protein separation. Journal of Membrane Science, 2013, 427(1): 155–167
2. Rohani M M, Mehta A, Zydney A L. Development of high performance charged ligands to control protein transport through charge-modified ultrafiltration membranes. Journal of Membrane Science, 2010, 362(1–2): 434–443
3. Kumar M, Ulbricht M. Low fouling negatively charged hybrid ultrafiltration membranes for protein separation from sulfonated poly(arylene ether sulfone) block copolymer and functionalized multiwalled carbon nanotubes. Separation and Purification Technology, 2014, 127: 181–191
4. Mehta A, Zydney A L. Permeability and selectivity analysis for ultrafiltration membranes. Journal of Membrane Science, 2005, 249 (1–2): 245–249
5. Kumar M, Ulbricht M. Novel antifouling positively charged hybrid ultrafiltration membranes for protein separation based on blends of carboxylated carbon nanotubes and aminated poly(arylene ether sulfone). Journal of Membrane Science, 2013, 448(50): 62–73
6. Kumar M, Ulbricht M. Novel ultrafiltration membranes with adjustable charge density based on sulfonated poly(arylene ether sulfone) block copolymers and their tunable protein separation performance. Polymer, 2014, 55(1): 354–365
7. Kumar R, Isloor A M, Ismail A F, Matsuura T. Synthesis and characterization of novel water soluble derivative of chitosan as an additive for polysulfone ultrafiltration membrane. Journal of Membrane Science, 2013, 440(1): 140–147
8. Xu J, Wang Z, Wang J X, Wang S C. Positively charged aromatic polyamide reverse osmosis membrane with high anti-fouling property prepared by polyethylenimine grafting. Desalination, 2015, 365: 398–406
9. Ba C Y, Economy J. Preparation and characterization of a neutrally charged antifouling nanofiltration membrane by coating a layer of sulfonated poly(ether ether ketone) on a positively charged nanofiltration membrane. Journal of Membrane Science, 2010, 362(1–2): 192–201
10. Ding N, Wang X L, Wang J. Electrokinetic phenomena of a polyethylene microfiltration membrane in single salt solutions of NaCl, KCl, $MgCl_2$, Na_2SO_4, and $MgSO_4$. Desalination, 2006, 192 (1–3): 18–24
11. Hanafi Y, Loulergue P, Ababou-Girard S, Meriadec C, Rabiller-Baudry M, Baddari K, Szymczyk A. Electrokinetic analysis of PES/PVP membranes aged by sodium hypochlorite solutions at different pH. Journal of Membrane Science, 2016, 501: 24–32
12. Furlán L T R, Campderrós M E. Effect of Mg^{2+} binding on transmission of bovine serum albumin (BSA) through ultrafiltration membranes. Separation and Purification Technology, 2015, 150: 1–12
13. AlMamuna M A A, Sadrzadeh M, Chatterjee R, Bhattacharjee S, De S. Colloidal fouling of nanofiltration membranes: A novel transient electrokinetic model and experimental study. Chemical Engineering Science, 2015, 138: 153–163
14. Wang L, Miao R, Wang X D, Lv Y T, Meng X R, Yang Y Z, Huang D X, Feng L, Liu Z W, Ju K. Fouling behavior of typical organic foulants in polyvinylidene fluoride ultrafiltration membranes: characterization from microforces. Environmental Science & Technology, 2013, 47(8): 3708–3714
15. Meng X R, Tang W T, Wang L, Wang X D, Huang D X, Chen H N, Zhang N. Mechanism analysis of membrane fouling behavior by humic acid using atomic force microscopy: effect of solution pH and hydrophilicity of PVDF ultrafiltration membrane interface. Journal of Membrane Science, 2015, 487: 180–188
16. Rahimpour A, Madaeni S S, Mansourpanah Y. Nano-porous polyethersulfone (PES) membranes modified by acrylic acid (AA) and 2-hydroxyethylmethacrylate (HEMA) as additives in the gelation media. Journal of Membrane Science, 2010, 364(1–2): 380–388
17. Wang X D, Zhou M, Meng X R, Wang L, Huang D X. Effect of protein on PVDF ultrafiltration membrane fouling behavior under different pH conditions: interface adhesion force and XDLVO theory analysis. Frontiers of Environmental Science & Engineering, 2016, 10(4): 1–11
18. Chang H Q, Liu B C, Luo W S, Li G B. Fouling mechanisms in the early stage of an enhanced coagulation-ultrafiltration process. Frontiers of Environmental Science & Engineering, 2015, 9(1): 73–83
19. Teli S B, Molina S, Calvo E G, Lozano A E, Abajo J D. Preparation, characterization and antifouling property of polyethersulfone-PANI/PMA ultrafiltration membranes. Desalination, 2012, 299: 113–122
20. Feng C S, Shi B L, Li G M, Wu Y L. Preparation and properties of microporous membrane from poly(vinylidene fluoride-co-tetrafluoroethylene) (F2.4) for membrane distillation. Journal of Membrane Science, 2004, 237(1–2): 15–24
21. Susanto H, Ulbricht M. Characteristics, performance and stability of polyethersulfone ultrafiltration membranes prepared by phase separation method using different macromolecular additives.

Journal of Membrane Science, 2009, 327(1–2): 125–135

22. Hwang G J, Ohya H. Preparation of anion-exchange membrane based on block copolymers: Part 1. Amination of the chloromethylated copolymers. Journal of Membrane Science, 1998, 140(2): 195–203
23. Kwon Y N. Change of surface properties and performance due to chlorination of crosslinked polyamide membranes. Dissertation for the Doctoral Degree. Palo Alto: Stanford University, 2006
24. Peula-Garcia J M, Hidaldo-Alvarez R, Nieves F J D L. Protein coadsorption on different polystyrene latexes: electrokinetic characterization and colloidal stability. Colloid & Polymer Science, 1997, 275(2): 198–202
25. Reuvers A J, Berg J W A V D, Smolders C A. Fomration of membranes by means of immersion precipitation. Part 1. A model to describe mass transfer during immersion precipitation. Journal of Membrane Science, 1987, 34(l): 45–65
26. Riedl K, Girard B, Lencki R W. Influence of membrane structure on fouling layer morphology during apple juice clarification. Journal of Membrane Science, 1998, 139(2): 155–166
27. Xu P, Drewes J E, Kim T U, Bellona C, Amy G. Effect of membrane fouling on transport of organic contaminants in NF/RO membrane applications. Journal of Membrane Science, 2006, 279(1–2): 165–175
28. Nyström M, Lindström M, Matthiasson E. Streaming potential as a tool in the characterization of ultrafiltration membranes. Colloids and Surfaces, 1989, 36(3): 297–312
29. Valiñoa V, Romána M F S, Ibáñeza R, Benitob J M, Escuderob I, Ortiz I. Accurate determination of key surface properties that determine the efficient separation of bovine milk BSA and LF proteins. Separation and Purification Technology, 2014, 135: 145–157
30. Palecek S P, Zydney A L. Intermolecular electrostatic interactions and their effect on flux and protein deposition during protein filtration. Biotechnology Progress, 1994, 10(2): 207–213
31. Nakao S, Osada H, Kurata H, Tsuru T, Kimura S. Separation of proteins by charged ultrafiltration membranes. Desalination, 1988, 70(1–3): 191–205
32. Miyama H, Tanaka K, Nosaka Y, Fujii N, Tanzawa H, Nagaoka S. Charged ultrafiltration membrane for permeation of proteins. Journal of Applied Polymer Science, 1988, 36(4): 925–933
33. Butt H J, Cappella B, Kappl M. Force measurements with the atomic force microscope: technique, interpretation and applications. Surface Science Reports, 2005, 59(1–6): 1–152
34. Krämer G, Griepentrog M, Bonaccurso E, Cappella B. Study of morphology and mechanical properties of polystyrene-polybutadiene blends with nanometer resolution using AFM and force-distance curves. European Polymer Journal, 2014, 55(6): 123–134
35. Celik E, Liu L, Choi H. Protein fouling behavior of carbon nanotube/polyethersulfone composite membranes during water filtration. Water Research, 2011, 45(16): 5287–5294